

# Partition Coefficients for a Mixture of Two Lubricant Oligomers

Vinod Kanniah,<sup>1</sup> T. Reg Forbus,<sup>2</sup> Stephanie Parker,<sup>2</sup> Eric A. Grulke<sup>1</sup>

<sup>1</sup>Chemical and Materials Engineering, University of Kentucky, Lexington, Kentucky 40506

<sup>2</sup>The Valvoline Company, Lexington, Kentucky 40509

Received 8 October 2010; accepted 30 November 2010

DOI 10.1002/app.34096

Published online 6 July 2011 in Wiley Online Library (wileyonlinelibrary.com).

**ABSTRACT:** Universal base oils that remain pourable over wide temperature ranges would have important advantages for lubrication applications. The model system used in this project was a poly( $\alpha$ -olefin) synthetic base oil modified with polydimethylsiloxane (PDMS) to lower the pour-point temperature. Although the blend was miscible at room temperature, phase separation occurred at temperatures lower than 258 K. Partition coefficients of such non-ideal oligomer mixtures can (1) help define operating temperature ranges and (2) provide a basis for designing molecular weight distributions of each lubricant that control or prevent phase separation. The poly( $\alpha$ -olefin) base oil family is branched oligomers with two to five *n*-mers at levels greater than 1 wt %, whereas PDMS additives are linear oligomers having between 10 and 50 sequential *n*-mers at levels greater than 0.5 wt %. In this study, Fourier transform infrared measurements of the poly( $\alpha$ -olefin) and PDMS compositions in each phase provided an

overall material balance. Poly( $\alpha$ -olefin) oligomers were detected with size exclusion chromatography with a differential refractive-index detector, and PDMS oligomers were detected with matrix-assisted laser desorption/ionization-time-of-flight mass spectrometry. The best sets of measurements for the individual oligomers in each phase were selected by minimization of the overall material balance errors. For both oligomers, components with high molecular weights were preferentially excluded from the phase rich in the other polymer and were relatively independent of temperature. The partition coefficients of poly( $\alpha$ -olefin) components increased with increasing oligomer length, whereas the partition coefficients of the PDMS components decreased with increasing oligomer length. © 2011 Wiley Periodicals, Inc. *J Appl Polym Sci* 122: 2915–2925, 2011

**Key words:** gel permeation chromatography (GPC); FT-IR; MALDI; oligomers; phase separation

## INTRODUCTION

$\alpha$ -Olefin oligomers, often called *poly( $\alpha$ -olefins)*, are commonly used as synthetic lubricant base stocks.<sup>1</sup> Poly( $\alpha$ -olefins) based on 1-decene oligomers (PAOs) have an extended range of operating temperatures relative to petroleum-based base oils and are a good starting point for the development of universal base oil products. Synthetic oils have excellent properties, including high viscosity indices, low pour points, and excellent shear stabilities. PAO commercial products with low kinematic viscosities are short-chain branched oligomers (dimers to heptamers) that have been hydrogenated to improve thermal stability.<sup>2</sup> Products with different kinematic viscosities are based on compositions with different sets of major *n*-mer components. For example, PAO2 (with a kine-

matic viscosity of 1.8 mm<sup>2</sup>/s at 100°C) has mostly dimer (99%) with some trimer, whereas PAO8 (with a kinematic viscosity of 7.9 mm<sup>2</sup>/s at 100°C) has mostly tetramer (56%) and pentamer (27%) with some trimer (6%), hexamer (7%), and heptamer (4%).<sup>2</sup>

There are several approaches to extending base oil use over a wider temperature range. One approach would be to vary the oligomer distribution and branching by modifying the polymerization process. A second approach would be to add a modest fraction of a lubricant that has improved low-temperature properties. Oligomer blends of two chemically different materials provide an interesting option for varying lubricant properties for a variety of applications. This work describes the measurement of the phase equilibria of such mixtures and the partition coefficients for the oligomer components between the two phases. The results can be used to tailor oligomers distributions so as to induce, or prevent, phase separation of binary oligomer mixtures over specific temperature ranges.

The specific model system, a mixture of 20 wt % polydimethylsiloxane (PDMS) in PAO6, had improved low-temperature viscosities compared to the PAO6 base oil product. PDMS oligomers have a high viscosity index (low variation with temperature)

Additional Supporting Information may be found in the online version of this article.

Correspondence to: E. A. Grulke (egrulke@engr.uky.edu).

Contract grant sponsors: US Army Tank Automotive Research, Development and Engineering Center (TARDEC).

and a comparatively low pour point, generally lower than 193 K. In contrast to the PAO family of products, the specific PDMS oligomer products used in this study contained a sequential series of linear n-mers having between 20 and 40 separable components. Different PDMS oligomer products have different average molecular weights; that is, they contain different distributions of n-mers. The PAO6/PDMS mixture is homogeneous at room temperature but separates at lower temperatures into a PAO6-rich continuous phase with PDMS-rich droplets.

### Partition coefficients

Phase equilibria for liquid–liquid systems are often based on fugacities or activity coefficients. At equilibrium, the fugacity ( $f$ ) of component 1 is the same in each of the two phases:

$$f_{1a}(T, P, x_a) = f_{1b}(T, P, x_b) \quad (1)$$

where  $x$  is the molar fraction; the subscripts  $a$  and  $b$  represent the top and bottom phases, respectively; and  $P$  is the pressure. Fugacity could be written in terms of an activity coefficient ( $\gamma$ ) as

$$f_1(T, P, x_a) = x_{a1}\gamma_{a1}(T, P, x_a)f_1(T, P) \quad (2)$$

For simple fluids, the activity coefficient is defined with the molar fraction as the concentration variable. However, volume fractions are usually more convenient for modeling polymer phase equilibria. The partition coefficient (the ratio of component concentrations in each phase) is equivalent to the activity coefficient ratio. Thus, the partition coefficient and activity coefficient for polymeric systems are related as follows:

$$\Phi_{1a}\gamma_{1a}(T, P, \Phi_a) = \Phi_{1b}\gamma_{1b}(T, P, \Phi_b) \quad (3a)$$

$$K_1 = \Phi_{1a}/\Phi_{1b} = \gamma_{1b}(T, P, \Phi_b)/\gamma_{1a}(T, P, \Phi_a) \quad (3b)$$

where  $\Phi$  is the volume fraction. There has been some prior work on partition coefficients for homologous series of oligomers related to polymer fractionation or changing solvents for polymerization and processing. Much of this research has focused on the use of supercritical fluids (e.g., carbon dioxide) or fluids near their critical points, where the solvency properties can be manipulated to control phase separation. For these systems, researchers have used a simple empirical model to describe the partitioning of individual components between the solvent-rich and polymer-rich phases.<sup>3</sup>

$$\ln(K_i) = \ln\left(\frac{w_i^s}{w_i^p}\right) = -\sigma n + \ln \xi \quad (4)$$

where  $K_i$  is the partition coefficient and is based on the weight fractions of component  $i$  distributed between the solvent-rich ( $w_i^s$ ) and polymer-rich phases ( $w_i^p$ ),  $\sigma$  is a separation factor that describes the dependence of  $K_i$  on the oligomer's chain length [degree of polymerization ( $n$ )], and  $\xi$  is a constant. For a relatively poor polymer solvent such as carbon dioxide, the oligomer component partition coefficients may decrease by several orders of magnitude as the chain length increases, and  $\sigma$  is a constant.<sup>3</sup> However, for liquid solvents<sup>4</sup> or for samples with very broad distributions,<sup>5</sup>  $\sigma$  may vary with chain length. In this study, the partition coefficients were based on volume fractions rather than weight fractions.

### Phase equilibria

Liquid–liquid equilibria of binary mixtures are usually expressed in terms of phase diagrams. In general, there are three ways of representing phase behavior, namely, a cloud-point curve (CPC), a coexistence curve, and a partition coefficient. The determination of the CPC for a system requires that a single-phase mixture be cooled or heated until the liquid becomes turbid or swells, that is, until it reaches its cloud point, which indicates the appearance of another phase. All the methods known for cloud-point determination require some amount of the second phase to be present so that the change can be detected.<sup>6</sup> The observed temperature may not be precise, and cloud-point temperatures are usually confirmed by more than one technique. Also, CPCs can depend on chain length and system pressure.<sup>7,8</sup> A coexistence curve describes the composition of each phase after separation for a known initial composition, but it is relatively tedious compared to CPCs. The simplest techniques for CPCs of polymer blends are turbidity and bottom-to-top phase volume ratio ( $r$ ) measurements,<sup>9</sup> which were used here.

The volume fractions of n-mers in each phase [eq. (3b)] were determined by measurement of the phase's total oligomer content and volume, and measurement of the relative amount of every n-mer. Matrix-assisted laser desorption/ionization (MALDI)–time-of-flight mass spectrometry (TOFMS)<sup>10</sup> was used to determine the relative distributions of the PDMS n-mers, whereas size exclusion chromatography (SEC)<sup>11</sup> was used to determine the relative distributions the poly( $\alpha$ -olefin) n-mers. Total oligomer contents were measured with Fourier transform infrared (FTIR) spectroscopy.<sup>12</sup> The reported data were shown to satisfy the overall material balances for each oligomer and the individual balances for every n-mer.

## EXPERIMENTAL

### Materials

The oligomer components of this study were PDMS (Chemical Abstracts Service Registry number (CAS Reg. no.) 42557-10-8, SK96-10, trimethylsilyl end groups, GE Silicones, USA) and poly( $\alpha$ -olefin) (CAS Reg. no. 68037-01-4, Chevron Phillips Chemical Co., LP, USA). PDMSs are commercially available with trimethyl, hydroxyl, and hydrogen end groups. The trimethyl end group products were chosen specifically to provide better compatibility with the poly ( $\alpha$ -olefin) base oils. The properties of the two oligomer systems are listed in Table S1 (see Supporting Information). The surface tension of the fluids was determined by the pendant drop technique with a goniometer (Model name: DSA10, KRUSS, USA). The refractive index was found with a refractometer (Bausch & Lomb, USA) with a sodium vapor lamp source. Dynamic viscosity of the fluids was determined with a concentric-cylinder-arranged rheometer (Model name: Viscoanalyzer, ATS Rheologica Instruments, USA). All of the neat fluids were Newtonian in the shear range of 1–1000  $\text{s}^{-1}$ , averaged over 15 data points within the temperature range 283–393 K.

### CPC

The CPC was determined through turbidity and phase volume ratio measurements. Turbidity measurements involved the cooling (or heating) of the sample and a record of the appearance (or disappearance) of turbidity with temperature. The samples were cooled in a refrigerated methanol bath maintained at 233 K. The cloud-point temperature was that at which the mixture turned clear from turbid (tests were run in triplicate). The cloud-point temperatures from the turbidity experiments were compared to those of the phase volume ratio method. A homogenized sample with a known initial composition was separated at a specific temperature, and its corresponding phase volumes were measured. The extrapolation of the phase volume curve to  $r = 0$  gave the cloud-point temperature. The exact time required for separation varied, depending on the temperature, molecular weight, and concentration of the oligomers. Hence, three samples of each composition were refrigerated for 48 h to ensure complete phase separation and settling. The volume of the top phase was measured with a graduated pipette (with 0.1 mL of precision). Care was taken to avoid intermixing of phases.

### SEC

Quantitative analysis of PAO6 was done with SEC. Three columns of mixed pore sizes (Styragel HR1 and Styragel HR2, Waters, Inc., and PL Gel Mixed E, Polymer Labs, Inc.) were used for efficient retention

(Table S2, see Supporting Information). Tetrahydrofuran (density = 0.889 g/mL at 295 K, High Performance Liquid Chromatography (HPLC) grade, Fischer Scientific, Inc.) was the standard eluent solvent for this instrument. A differential refractive-index detector (model 2410, Waters) was used. An auto sampler (SIL-20A HT, Shimadzu, Inc.) was used for the samples. The column conditions used were as follows: volumetric flow rate = 1 mL/min, column temperature = 313 K, injection volume = 20  $\mu\text{L}$ , and refractive-index detector sensitivity = 128.

PDMS/PAO6 blends of 0.179 volume fraction [ $v/(v + v)$ ] PDMS were phase-separated at three temperatures (233, 243, and 258 K). After centrifuging, samples of the top and bottom phases were drawn via syringe and diluted with THF. Care was taken to prevent intermixing of phases during sampling. The total cycle time was set to 10 min greater than the sample elution time to ensure that the columns were completely flushed before the next injection.

### MALDI-TOFMS

MALDI-TOFMS experiments were performed to determine the molecular weight distribution of the PDMS oligomer. MALDI mass spectra were obtained in a linear mode on a Bruker Daltonics autoflex time-of-flight (TOF) mass spectrometer (Billerica, MA) with a 2,5-dihydroxybenzoic acid (DHB) matrix. The DHB matrix was used for analysis of polymer mixtures containing PDMS and PMMA with MALDI-TOFMS.<sup>10</sup> The matrix and conditions of Yan et al.<sup>10</sup> appeared to give relative signal intensities adequate for quantitative measurements of the various oligomers. A thin film technique of sample preparation was used. DHB matrix dissolved in a 50 wt % methanol–water mixture was deposited on the sample carrier. Once the solvents evaporated, the analyte solution samples were then deposited over the dry matrix. Analyte samples were made to a concentration of 1 mg/mL in dichloromethane. Instrument conditions were as follows: voltage extractions (IS1, 20 kV, and IS2, 18.65 kV), lens (8.25 kV), pulsed ion extraction (50ns), matrix suppression (gating, medium), and up to 650 Da. Neat PDMS samples and samples from PDMS-rich phases gave almost reproducible data when they were hit by varying laser shots (100–200). However, samples from PAO6-rich phases required 200 laser shots for consistent results. All data reported for partition coefficient estimates used 200 laser shots because the absolute intensity of the MALDI signal was affected by the laser and matrix crystallization conditions. The data obtained was thus optimized for these samples on the basis of a good signal-to-noise ratio (i.e., signal standing out of the background) and good mass resolution (i.e., narrow peak width).



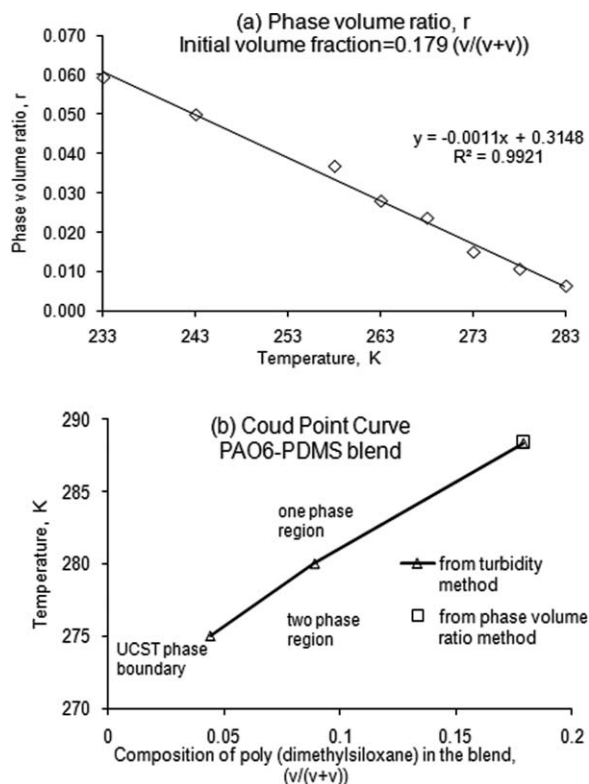


**Figure 1** (a) Phase volume ratio versus temperature [( $\diamond$ ) data and (—) trend line] and (b) CPC of the PAO6–PDMS blend [(— $\triangle$ —) turbidity method data and ( $\square$ ) phase volume ratio method data].

### Overall phase composition: FTIR spectroscopy

FTIR spectroscopy was used to determine the total PDMS and PAO6 concentrations in each phase of the separated mixtures. A NEXUS 470 FTIR spectrometer with an attenuated total reflection accessory, a ZnSe window, and a Deuterated Triglycine Sulfate (IR detector material) (DTGS) KBr detector were used.

## RESULTS AND DISCUSSION

CPCs were measured to establish the extent of separation on the bases of temperature and composition. Different measurement techniques were used for each oligomer family, as no single tool could detect both materials simultaneously. For example, their molecular weight ranges overlapped, so SEC data would need to be deconvoluted on the bases of two different curve shapes. FTIR spectroscopy was used to measure the total amount of oligomer in the separated phases. This approach provided n-mer volume fraction data confirmed by material balances. The n-mer partition coefficient data of each oligomer family were compared to eq. (4), which has been used to model n-mer partitioning data for other applications, such as polymer fractionation and polymerization solvent replacement.

### CPC

The CPC and phase volume ratio for a volume fraction of PDMS oligomer  $\{= 0.179 [v/(v + v)]\}$  in the blend are shown in Figure 1. Figure 1(a) corresponds to the phase volume ratio, and Figure 1(b) corresponds to the CPC of the system. As the temperature was lowered, the amount of PDMS miscible with PAO6 decreased. The phase volume ratio of the oligomer mixture showed the extent of separation possible at those temperature and compositions. The cloud-point temperature obtained by extrapolation of the phase volume ratio to temperature was close to the temperatures obtained through turbidity methods; this verified the measurements as reasonable values.

### Quantitative analysis for PAO6 n-mers

PAO6 n-mers were easily detected by an SEC column because of the large difference between their refractive index and that of the solvent [ $n_d = 1.4570$  (PAO6) vs  $n_d = 1.4072$  (THF)]. PDMS oligomers went undetected by refractive-index detectors [ $n_d = 1.3999$  (PDMS); Fig. 2] and ultraviolet–visible and fluorescence detectors. The apparent molecular weight range of the two oligomer systems overlapped. PAO6 branched oligomers eluted with apparent molecular weights of about 580 Da to about 1400 Da. The linear PDMS oligomers had a molecular weight range from about 600 Da to about 3300 Da. These ranges overlapped (as shown in Fig. S1, Supporting Information); this greatly complicated the interpretation of the SEC data. The use of a specific analytical tool for each oligomer type eliminated potential interferences but required the use of an overall material balance to select the most accurate measurements.

### SEC column calibration

The SEC column was calibrated with nine linear polystyrene standards [ $580 < \text{weight-average molecular weight } (M_w) < 19,880$ ]. The  $\log M_w$  versus retention time plot was linear [ $R^2 = 0.994$ , Fig. 3(a)]

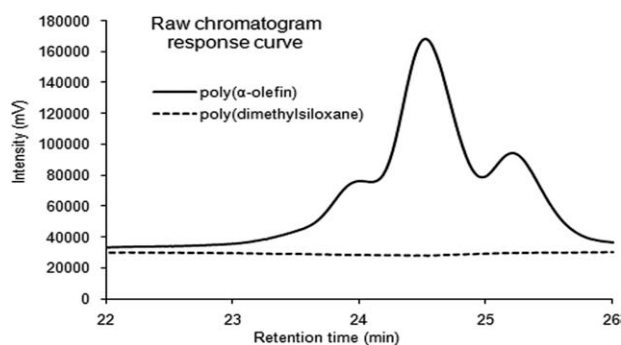


**Figure 2** Raw chromatogram response curve of the PAO6 and PDMS oligomers as obtained: (—) PAO6 and (---) PDMS.

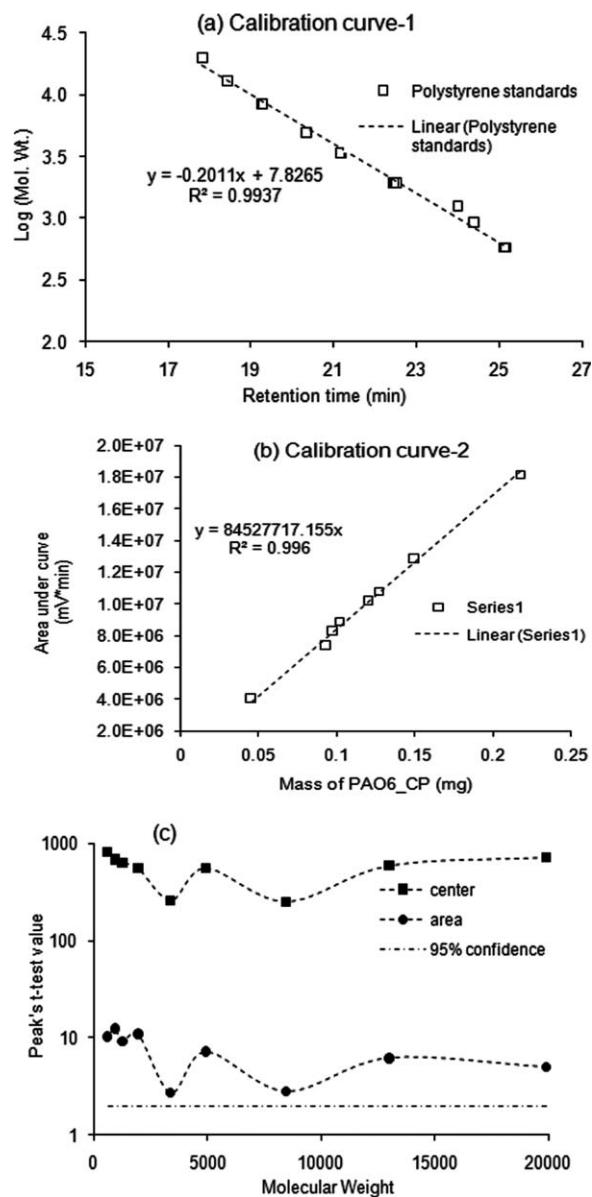


**Figure 3** Calibration curves with linear polystyrene standards: (a) molecular weights versus retention times, (b) peak area versus sample mass [(□) data and (- - □ - -) trend line], (c) peak *t*-test values [(●) area, (■) center, and (- - -) 95% confidence; *y* axis on the logarithmic scale].

as was the plot of peak area versus oligomer mass [ $R^2 = 0.996$ , Fig. 3(b)]. Several statistical models were evaluated (lognormal, modified Gaussian, and exponentially modified Gaussian), but the Gaussian area was chosen on the basis of its simplicity and fit to the data. Gaussian area or normal distribution [eq. (5)] has three parameters: area under the curve [ $A_0$  (peak area)], mean [ $A_1$  (peak center)], and standard deviation [ $A_2$  (peak width)]:

$$y = \frac{A_0}{\sqrt{2\pi}A_2} \exp\left[-\frac{1}{2}\left(\frac{x - A_1}{A_2}\right)^2\right] \quad (5)$$

where *y* is the relative intensity corresponding to each data point (molecular weight) in a peak. The maximum percentage variations allowed for parameter estimates were set to  $A_0$  (25%),  $A_1$  (1%), and  $A_2$  (25%), respectively. These functions were converged numerically through least-squares minimization to obtain parameter estimates. When a specific distribution model is selected, the student *t*-test parameter can be used to evaluate the quality of fit, specifically, the location of the center of the peak and the peak area. For the linear polystyrene standards, the *t*-test values for peak centers and peak areas greatly exceed the 95% confidence value [Fig. 3(c)], particularly for molecular weights less than 3000 Da. The high *t*-test value for peak centers is due, in part, to the low tolerance permitted for coefficient  $A_1$  in the fitting procedure.

#### Identification of the PAO6 *n*-mer peaks

The low-molecular-weight PAO family of lubricants is produced by the polymerization of 1-decene to oligomers with a  $\text{BF}_3$  catalyst system followed by hydrogenation.<sup>2</sup> NMR data show that an extra branch exists for such oligomers, which is thought to be caused by a skeletal rearrangement of the oligomers.<sup>13</sup> A typical composition of PAO6 is shown in Table I.<sup>14</sup> Trimer, tetramer, and pentamer are its major components (94 wt %), and hexamer, heptamer, and dimer are its minor components (<6 wt %). Commercial PAO6 samples would be expected to have the same major components (trimer, tetramer, and pentamer); therefore, the major peaks should be the same, even with typical lot-to-lot variations.

SEC chromatographs of neat PAO6 were deconvoluted with commercial software (Peak Fit Version 4.12) to determine the percentage area contributed by each peak [Fig. 4(a)]. Three major peaks and two minor peaks were observed (Table I) and were assumed to be trimer, tetramer, pentamer, hexamer, and heptamer in their elution order. A small lead peak (dimer) was not detected. The hydrogenated *n*-mers should have had actual molecular weights that were nearly integer multiples of the monomer values, that is, 280, 420, 560, 700, 840, and 980 for dimer through heptamer, respectively. However, the apparent molecular weights (peak centers) of the PAO6 oligomers were higher than their nominal molecular weights. This peak assignment correctly described another poly( $\alpha$ -olefin), PAO4, as shown in Table I.

SEC separations are based on the hydrodynamic radii of the macromolecules, which vary with the chemical composition of the chain and its configuration (e.g., linear, branched, star). A number of factors could cause PAO6 oligomers to have higher than expected hydrodynamic radii. A molecular dynamics

TABLE I  
Chemical Composition of the Two Poly( $\alpha$ -olefin)s

Component (nominal $M_w$ )	PAO6 peak center <sup>a</sup>	PAO6 (wt %) <sup>a</sup>	PAO6 (wt %) <sup>2</sup>	PAO4 peak center <sup>b</sup>	PAO4 (wt %) <sup>b</sup>	PAO4 (wt %) <sup>2</sup>
Dimer (280)	—	—	0.1	—	—	0.6
Trimer (420)	582	22.5	33.9	548	84.9	84.4
Tetramer (560)	792	55.1	43.5	759	15.1	14.5
Pentamer (700)	1018	17.5	17.4	—	—	0.5
Hexamer (840)	1224	4.19	3.8	—	—	—
Heptamer (980)	1413	0.74	1.3	—	—	—

<sup>a</sup> Data in Figure 5.

<sup>b</sup> Analysis of data in Figure S2 (see Supporting Information).

study of the effective dimensions of oligomers in SEC showed that the effective hard-sphere radii (the retention radii) of molecules of less than 5000 Da were larger than their radii of gyration.<sup>15</sup> Furthermore, different polymers had different retention radii, which were attributed to the asphericities of their individual configurations. Trimers, tetramers, and pentamers based on 1-decene have branch lengths that are similar in size to the chain backbone and can be categorized as star-type molecules. The SEC data of some star-type oligomers (2000 Da < number-average molecular weight < 5500 Da)

showed much higher (40–100%) apparent molecular weights.<sup>16</sup> Because this was a homologous sequence of oligomers polymerized by the same catalyst, there was likely to be a consistent relationship between the apparent molecular weight and the actual molecular weight. A power law relation was used as an empirical model:

$$M_{w_{app}} = a(M_{w_{n-mer}})^b \quad (6)$$

where  $M_{w_{app}}$  is the apparent molecular weight determined by SEC analysis,  $a$  is a constant,  $M_{w_{n-mer}}$  is the expected molecular weight of the  $n$ -mer, and  $b$  is the exponent. For the five  $n$ -mers shown in Table I, the constant value was 0.65, the exponent was 1.12, and the correlation had an  $R^2$  value greater than 0.999. This correlation was consistent with the known  $n$ -mers of PAO6 and with the typical apparent  $M_w$  values for branched molecules in SEC.

Figure 4(b) shows the  $t$ -test values (ratio of the parameter estimate to its average standard error) for the PAO6  $n$ -mer peak centers and peak areas. The dash-dot line on the graph is the  $t$ -test values of an infinite number of data points for which 95% of all populations would have the same mean. The peak center  $t$ -test values were an order of magnitude higher than the peak area  $t$ -test values. Because the peak area  $t$ -test values for the hexamer and heptamer were below the 95% significance line, only the trimer, tetramer, and pentamer were considered for partition coefficient analysis.

#### Poly( $\alpha$ -olefin) in separated phases

The molecular weight distribution of PAO6 in separated phases from a blend of initial volume fraction of 0.179 at 258 K is shown in Figure 5. These distributions showed the relative oligomer amounts in each phase; the volume fraction of oligomer was determined with the material balance. The bottom phase (rich in PDMS) was enriched in the trimer and lean in the pentamer. The top phase (rich in PAO6) was enriched in the pentamer and lean in the trimer.

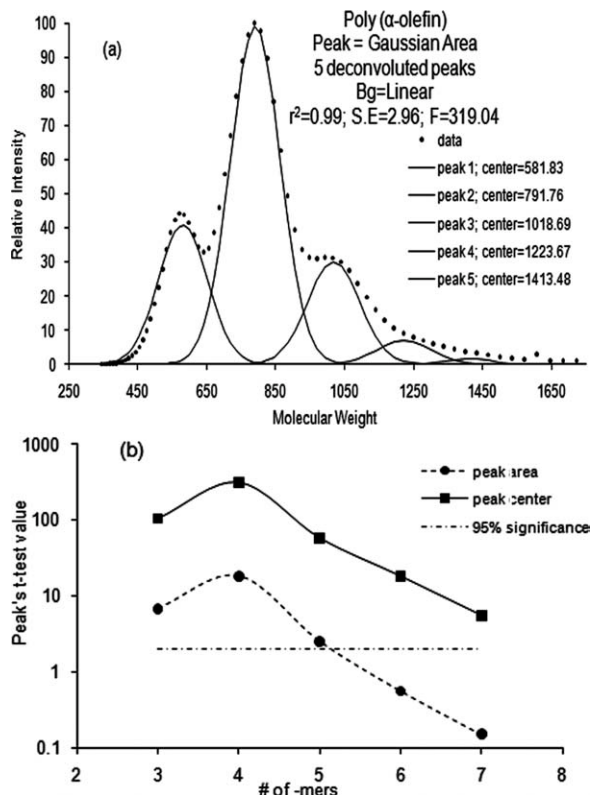


**Figure 4** Neat PAO6 oligomer data fit to (a) Gaussian area distribution [(●) data and (—) peaks 1–5], (b) peak  $t$ -test values [(—●—) peak area, (—■—) peak center, and (—·—) 95% confidence;  $y$  axis on the logarithmic scale; S.E. = standard error;  $F$  =  $F$  statistic value].



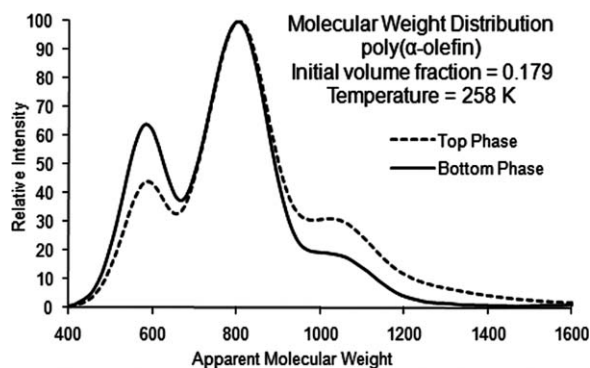


**Figure 5** PAO6 volume fractions in the top and bottom phases.  $T = 258$  K. Initial volume fraction of the blend = 0.179 [ $v/(v + v)$ ] of the PDMS oligomer. (---) top phase and (—) bottom phase.

### Quantitative analysis for PDMS oligomers

#### Identification of PDMS n-mer peaks

The PDMS repeating unit had a molecular weight of 74.08; MALDI-TOF analysis data of the PDMS samples with sequential oligomers having the same end groups should have had about 74-Da spacing between each sequential n-mer pair. The PDMS sample selected for this study had the molecular weight differential between oligomers that was closest to the theoretical value and had few missing n-mers in the sequence. Samples from other suppliers were considered but either had some n-mers missing from the sequence or presented other deviations from the expected molecular weight series.

Figure 6 shows peaks from a MALDI-TOF analysis of neat PDMS. The nominal molecular weight of PDMS oligomers with trimethyl silyl end groups was  $n \times 74.08$  plus the molecular weight of the end groups (88.1 Da). Overlaid on the peaks of Figure 6 are a set of bars spaced by 74.08 Da covering the range  $600 \text{ Da} < M_w < 3000 \text{ Da}$ . For sequential oligomers such as this PDMS sample, MALDI-TOF

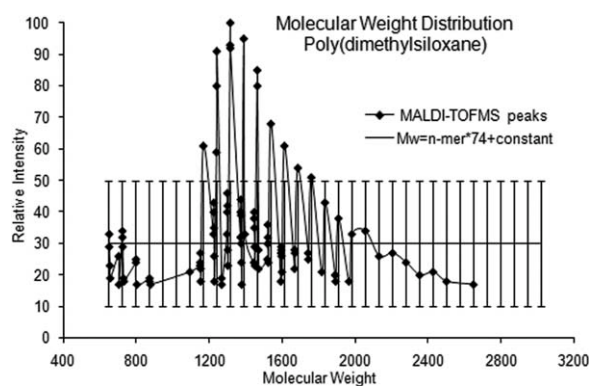


**Figure 6** Cumulative frequency versus the molecular weight for the neat PDMS n-mers: (◆) MALDI-TOF peaks. The bar overlay shows peaks separated by 74.08 Da.

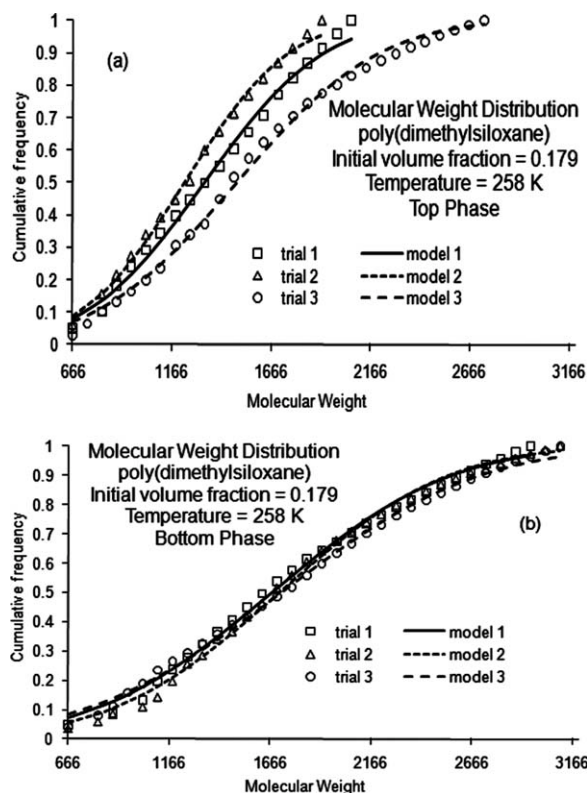


**Figure 7** Effect of the number of laser shots on PDMS n-mer detection. Cumulative molecular weight distributions of (a) top phase and (b) bottom phase. Initial volume fraction of blend = 0.179 [ $v/(v + v)$ ] of the PDMS oligomer. Phase-separation temperature = 258 K. (□) trial 1, (△) trial 2, (○) trial 3, (—) model 1, (---) model 2, and (- - □) model 3.

provides precise differences between the molecular weights of nearby n-mers. Because of the nature of the analysis, additional molecular fragments may be generated, which make the peak position different from the precise molecular weight of the n-mer. This set of bars was displaced from the expected n-mer molecular weights ( $M_w = n \times 74.08 \text{ Da}$ ) by 55 Da, but it matched peaks over the entire range. The standard deviation between the peak molecular weight and the nominal molecular weight was  $\pm 1.06$  Da over the range 600–3300 Da. This differential distribution was used to compute the sample's average molecular weight (1781 Da), which compared well to the manufacturer's reported value (1790, Table S1, see Supporting Information).

#### Laser power for spectral quality

Figure 7(a,b) shows the cumulative frequency curves for the PDMS oligomer in the top and bottom phases for three replicate samples analyzed with different numbers of laser shots. Trials 1 and 2 were each analyzed with 100 laser shots, whereas trial 3 used 200 laser shots. Although replicate data sets for the

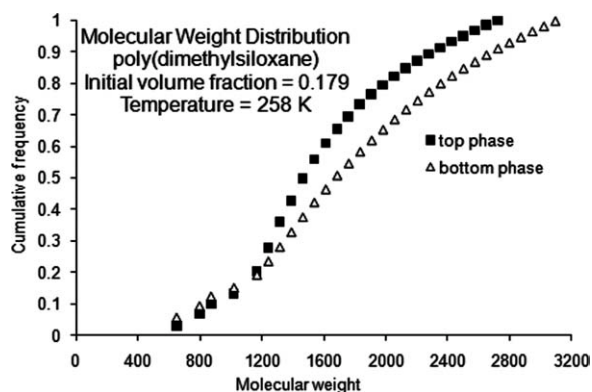


**Figure 8** PDMS volume fractions in the top and bottom phases.  $T = 258$  K. Initial volume fraction of the blend = 0.179 [ $v/(v + v)$ ] of the PDMS oligomer. (■)  $N$ -mer volume fractions in the top phase and (△)  $n$ -mer volume fractions in the bottom phase.

200-laser-shot method are not shown, this technique provided very consistent data, and the method was used for the PDMS analysis. Figure 8 describes the volume fraction of PDMS in the top and bottom phases at 258 K. Less accurate data sets were obtained for the PDMS oligomer in the top phase, which typically contained about 8 vol % PDMS compared to 84 vol % PDMS in the bottom phase.

The matrix method<sup>10</sup> has been shown to properly analyze PDMS  $n$ -mers in the range  $6 < n < 40$ . Oligomers with different chain lengths have similar ionization/desorption probabilities even in the presence of a third polymer. This method provides relative differential distributions of oligomers,<sup>10</sup> which, when combined with overall material balances, can be used to determine individual component concentrations in a solution with the assumption of no volume changes on mixing. Other researchers<sup>17,18</sup> have also reported that the MALDI-TOF MS method does not demonstrate sensitivity differences for high-mass oligomers. However, for PDMS  $n$ -mer chains less than 12 repeating units long,<sup>18</sup> there appears to be some sample loss when MALDI-TOF results are compared directly with supercritical fluid chromatography.<sup>19</sup> This reduction does not seem to be associated with PDMS oligomer fragments undergoing metal-catalyzed reactions during the laser ablation process.<sup>19</sup> Because these losses for  $n$ -mers with  $n \leq 12$  should be similar from sample to sample, the relative differential distributions should not be affected much and were used in combination with material balances to determine the PDMS  $n$ -mer concentrations in each phase.

## Overall material balance

### FTIR peak selection

The peaks for the quantitative analysis of PDMS and PAO6 in separated phases were selected to have

minimal interference with each other. The FTIR absorbance spectra of neat PDMS and neat PAO6 liquids are shown in Figure 9, where they are plotted as absorbance versus wave number ( $\text{cm}^{-1}$ ). The solid line spectrum corresponds to PAO6, and the dashed line spectrum corresponds to PDMS. A blend of the oligomers with a 0.179 volume fraction of PDMS is shown as a dashed dotted line. Two distinct peaks were chosen each for oligomer [PDMS: (A) 1257 and (B) 1040  $\text{cm}^{-1}$ ] and [PAO6: (C) 1462 and (D) 2852  $\text{cm}^{-1}$ ]. The PAO6 oligomer peak at 2852  $\text{cm}^{-1}$  corresponded to the stretching vibration of methyl groups ( $-\text{CH}_3$ ) or methylene groups ( $-\text{CH}_2-$ ). The peak at 1462  $\text{cm}^{-1}$  corresponded to the bending vibration of  $-\text{CH}_2-$  groups.<sup>20</sup> PDMS had a sharp peak near 1040  $\text{cm}^{-1}$ , which corresponded to symmetrical Si—O—Si stretching,<sup>21</sup> whereas the narrow peak at 1257  $\text{cm}^{-1}$  corresponded to asymmetric C—Si—O stretching.<sup>22</sup> Peaks were selected with a high response for the target molecule and a low or nonchanging baseline of the other type of molecule. Baselines were established for each peak, and both peak height and peak area were considered for quantitative analysis.

Three spectra were obtained for each volume fraction to check repeatability. It was evident that peak area was better than peak height for quantitative analysis of these oligomers. The calibration curves were nonlinear for either peak area or peak height as the measure, and second-order polynomial fits provided the best  $R^2$  ( $>0.99$ ). Peak A was the best for PDMS oligomer, and peak C was taken to be the best choice for the PAO6 oligomer calibration curve.

## Material balance evaluations

Phase-separated samples (top and bottom) at 233, 243, and 258 K were analyzed via FTIR spectroscopy. The volume fractions of PDMS oligomer in the demixed samples were obtained through FTIR quantitation at 1257  $\text{cm}^{-1}$  (peak A for PDMS oligomer

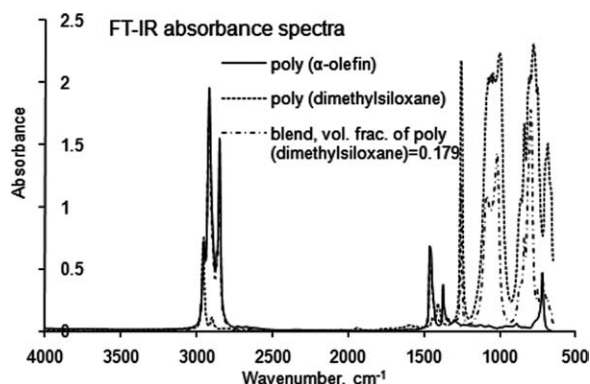


**Figure 9** FTIR absorbance spectra of the (---) neat PDMS, (—) neat PAO6, and (- · - ·) a blend: volume fraction of PDMS = 0.179.



**TABLE II**  
Phase Equilibria Data via FTIR Analysis

Phase	PAO6_CP [ $v/(v + v)$ ]	PDMS_GE [ $v/(v + v)$ ]
Temperature = 258 K		
Top	<i>0.746 ± 0.094</i>	<i>0.141 ± 0.008</i>
Bottom	<i>0.083 ± 0.035</i>	<i>0.91 ± 0.331</i>
Temperature = 243 K		
Top	<i>0.834 ± 0.038</i>	<i>0.135 ± 0.004</i>
Bottom	<i>0.084 ± 0.016</i>	<i>0.918 ± 0.083</i>
Temperature = 233 K		
Top	<i>0.876 ± 0.011</i>	<i>0.125 ± 0.005</i>
Bottom	<i>0.087 ± 0.029</i>	<i>0.983 ± 0.191</i>

Preferred data are in italic font.  
CP = Chevron Phillips; GE = GE silicone.

through second degree polynomial fit) and  $1462 \text{ cm}^{-1}$  (peak C for PAO6 oligomer through linear fit; see Table II). The volume fractions of PAO6 oligomer in the samples were then determined by subtraction of PDMS oligomer volume fractions from 1. All of the volume fractions are reported with a 95% confidence interval ( $\pm 2$  standard deviations) determined through three repetitions in Table S1 (see Supporting Information). The most accurate experimental data (analyses of the leanest component in the phase) are shown in italic print, that is, these data closed the material balance within 5%. For example, the best volume fraction data for the top phase was PDMS oligomer, whereas the best volume fraction data for the bottom phase was PAO6 oligomer.

Overall and component material balances were needed to determine the partition coefficients for the various mixture components. A material balance check was performed for all three temperatures (233, 243, and 258 K) data to evaluate the accuracy of the characterization techniques chosen. The oligomer volumes in the separated phases were computed by multiplication of the volume fractions in each phase with the phase volumes. The difference between the volumes of oligomer used in the mixture to those measured in the separated phases was best (the raw data was evenly distributed about zero) when volume fractions measured by FTIR spectroscopy were used.

### Partition coefficients

Modeling the partition coefficient of PAO6 ( $K_{\text{PAO6}}$ )

Partition coefficient estimates were based on the data sets with the best closure of overall and oligomer material balances. Figure 10 shows partition coefficient estimates for PAO6 n-mers phase-separated at three different temperatures, 233, 243, and 258 K.  $K_{\text{PAO6}}$  increased as the degree of polymerization increased but was not sensitive to tem-

perature over this temperature range. The fitting coefficients of eq. (4) were  $\sigma = 0.395 \pm 0.026$  and  $\ln \xi_i = 0.712 \pm 0.118$ , with an  $R^2$  value of 0.975. The partition coefficient data for the hexamer are also shown, even though the values of their peak areas by SEC did not meet the quality criteria [Fig. 5(b)]. In this case, the hexamer partition coefficients appeared to conform to the simple model. The heptamer data did not conform to eq. (4), but there were wide variations in the partition coefficient values (consistent with the low quality of the peak area data).

Consider the phase equilibria concentrations at a specific temperature ( $T = 243 \text{ K}$ ). Over 99% of the PAO6 n-mers in the mixture were in the top phase. If we assumed an extrapolated partition coefficient for the hexamer (Fig. 10), over 99.8% of this n-mer was in the top phase. By contrast, 79% of the PDMS in the mixture was in the top phase, with the remainder in the bottom phase.

There have been a few articles on the partitioning of oligomers into supercritical carbon dioxide that have developed simple<sup>3</sup> and equation-of-state models.<sup>23,24</sup> In general, supercritical carbon dioxide is not a good solvent for polymeric oligomers, and longer chain lengths have significantly lower solubilities. For example, the partition coefficients for styrene oligomers in carbon dioxide can decrease several orders of magnitude as the molecular weight increases from 1000 to 2000 Da.<sup>3</sup> The partition coefficients are not particularly sensitive to temperature changes, as the carbon dioxide phase fluid density is not particularly sensitive to temperature. Equation (4) is appropriate for a linear combination of independent, quasi-binary systems of supercritical carbon dioxide with individual oligomers. Equation (4) also seemed to be a satisfactory model for the partitioning of the PAO6 n-mers in the mixture.

Equation (4) suggests that the trimer and tetramer have lower values for the partition coefficient.

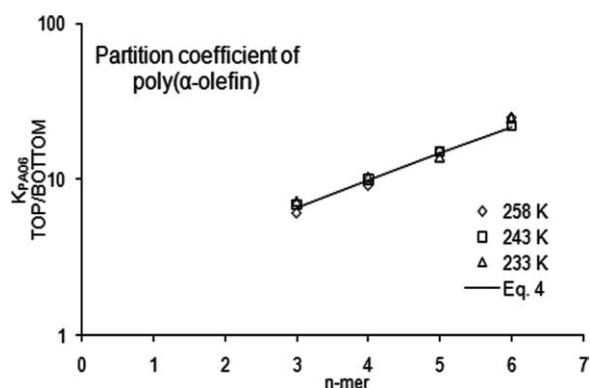


**Figure 10** Partition coefficient estimates for the PAO6 oligomer.  $T = (-\triangle-\triangle-)$  258,  $(-\square-\square-)$  243, and  $(-\diamond-\diamond-)$  233.

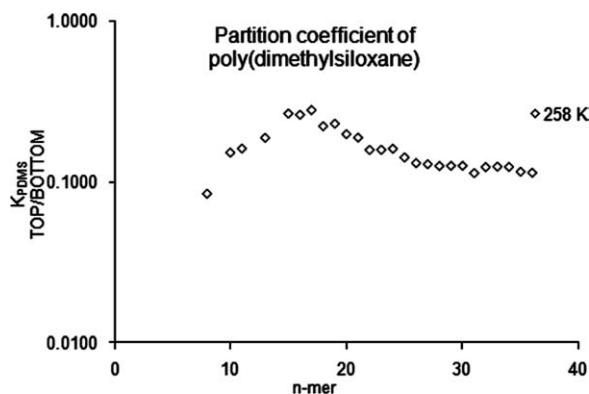


**Figure 11** Partition coefficient estimates for the PDMS oligomer. ( $\diamond$ ) partition coefficient (top/bottom) data at 258 K.

Therefore, a PAO sample enhanced in these components and depleted in pentamer and hexamer should be more soluble than PAO6 in a PAO/PDMS mixture. This hypothesis was easily tested, as PAO4 (Table I) has about 84% trimer, 14% tetramer, and very little higher  $n$ -mers. Mixtures of PAO4 in PDMS did not phase-separate at temperatures down to 233 K; this showed that this simple correlating tool might be helpful in the development of mixtures of oligomers with specific phase-separation characteristics.

#### Modeling the partition coefficient of PDMS ( $K_{\text{PDMS}}$ )

There are examples of supercritical fluid/oligomer partition coefficients that no longer follow a straight line on a log-linear plot of  $K_i$  versus  $X_i$ . These include polystyrene in better solvents (ethane and propane)<sup>3</sup> and poly(vinylidene fluoride) in carbon dioxide (a polar polymer in a polar solvent).<sup>23</sup> Figure 11 shows  $K_{\text{PDMS}}$  values of the PDMS oligomer components versus molecular weight at 258 K. The  $n$ -mer partition coefficients went through a maximum and then declined as chain length increased for  $n \geq 17$ . Equation (4) is not a good model for this behavior, even for longer chain lengths. The presence of a modest maximum in oligomer partition coefficients has occurred with other systems, such as the phase behavior of Poly(vinylidene fluoride) (PVDF) oligomers in carbon dioxide near the critical point.<sup>24</sup> Bonavoglia et al.<sup>24</sup> modeled their data with the Sanchez-Lacombe equation of state by allowing the interaction parameter ( $\chi$ ; normally considered to be a constant) to vary with chain length. Although empirical, this approach demonstrated that additional terms would be needed in the fitting parameter to describe the data.

As  $K_{\text{PDMS}}$  is computed directly from volume fractions, it was convenient to use the Flory-Huggins model to model the partitioning between PAO6 and

PDMS  $n$ -mers. Flory-Huggins theory has been applied to several polydisperse binary and quasi-binary polymer systems but has been applied to only a few phase-separated polydisperse binary polymer mixtures, for example, a phase-separated mixture of gelatin and dextran.<sup>25</sup> This system had moderate levels of two polymers in a common solvent. They used 5 wt % of each monomer in the mixture, for which the  $n$ -mer lengths ranged from 500 to 1000. They found that the degree of fractionation (equivalent to the partition coefficients reported here) was a function of  $n$ -mer length and that the scaling was well-described by a model similar to Eq. (4) and Flory-Huggins theory. The conventional Flory-Huggins equations for phase separation, written for an  $n$ -mer, are

$$\ln \left( \frac{\phi_{n,\text{PDMS}}^T}{\phi_{n,\text{PDMS}}^B} \right) = N \left[ \frac{1-N}{N} \left[ \left( 1 - \phi_{n,\text{PDMS}}^B \right) - \left( 1 - \phi_{n,\text{PDMS}}^T \right) \right] + \chi \left[ \left( 1 - \phi_{n,\text{PDMS}}^B \right)^2 - \left( 1 - \phi_{n,\text{PDMS}}^T \right)^2 \right] \right] \quad (7)$$

where  $\phi_{n,\text{PDMS}}^j$  is the volume fraction of oligomer  $n$ -mer in the  $j$ th phase (where the superscript  $T$  indicates the top phase and the superscript  $B$  indicates the bottom phase) and  $N$  is the molar volume ratio and is estimated with  $n$  (or the molar volume ratio of the  $n$ -mer to the solvent phase). The left-hand side of eq. (7) is the volume fraction partition coefficient. In this case, eq. (7) could only be considered a correlating tool, as both oligomer systems appeared to have chain length-dependent partition coefficients. The values of  $\chi$  for both oligomers showed minima with chain length. Components with low values of  $\chi$  usually are interpreted as having better solubility in phase-separating systems. Among the PAO6  $n$ -mers, the tetramer had the lowest value for  $\chi$ ; this suggested that it would be most soluble in PDMS. Among the PDMS  $n$ -mers with chain length between 16 and 22 appeared to have local minima in  $\chi$ ; this suggested that these would be most soluble in PDMS. The first of these hypotheses was easily tested, as PAO4 (Table I) had about 84% tetramer. In this case, the Flory-Huggins model did not scale in an analogous fashion to eq. (4), and a more complex model would be needed.

## CONCLUSIONS

Partition coefficient estimates for individual oligomer components were determined by separate analytical methods for PAO6 (SEC-Differential Refractive Index (DRI)) and PDMS (MALDI-TOFMS),

which were linked with overall material balance measurements (FTIR spectroscopy). Partition coefficients of the PAO6 components increased with increasing oligomer components and were relatively independent of temperature. The partition coefficients of the PDMS components decreased with increasing oligomer components. For both oligomers, components with high molecular weights were preferentially excluded from the phase rich in the other polymer. The partition coefficient data could be used to develop oligomers with different distributions of component chain lengths that would have different cloud points. This could be done by the control of the oligomer chain lengths during polymerization, fractionation of existing commercial materials, addition of monodisperse components, or via combinations of these methods.

As the authors are not government employees, this document was only reviewed by Operations Security (OPSEC) for export controls and improper U.S. Army association or emblem usage considerations. All other legal considerations are the responsibility of the authors. The authors thank Jack Goodman of the Chemistry Department for assistance with the MALDI-TOF analysis.

## References

1. Pirro, D. M.; Wessol, A. A. *Lubrication Fundamentals*; Marcel Dekker: New York, 2001.
2. Voelkel, A.; Fall, J. *J Synth Lubrication* 2007, 24, 91.
3. Kumar, S. K.; Chhabria, S. P.; Reidand, R. C.; Suter, U. W. *Macromolecules* 1987, 20, 2550.
4. Schulz, G. V.; Jirgensons, B. Z. *Phys Chem B* 1940, 46, 105.
5. Koningsveld, R.; Stockmayer, W. H.; Kennedy, J. W.; Kleintjens, L. A. *Macromolecules* 1974, 7, 73.
6. Coutinho, J. A. P.; Daridon, J. L. *Pet Sci Technol* 2005, 23, 1113.
7. Koningsveld, R.; Staverman, A. J. *J Polym Sci Part A-2: Polym Phys* 1967, 6, 305.
8. Imre, A. R. *Polym Sci* 2003, 21, 241.
9. Borchard, W.; Frahn, S.; Fischer, V. *Macromol Chem Phys* 1994, 195, 3311.
10. Yan, W.; Gardella, J. A.; Wood, T. D. *J Am Soc Mass Spectrom* 2002, 13, 914.
11. Narasimhan, V.; Lloyd, D. R.; Burns, C. M. *J Appl Polym Sci* 1979, 23, 749.
12. Chen, J.; Gardella, J. A. *Appl Spectrosc* 1998, 52, 361.
13. Shubkin, R. L.; Baylerian, M. S.; Maler, A. R. *Ind Eng Chem Prod Res Dev* 1980, 19, 15.
14. Shubkin, R. L. *Polyalphaolefins*; CRC: London, 1994.
15. Boyd, R. H.; Chance, R. R.; Ver Strate, G. *Macromolecules* 1996, 29, 1182.
16. Helminen, A.; Korhonen, H.; Seppala, J. V. *Polymer* 2001, 42, 3345.
17. Chmelik, J.; Konecny, P.; Planeta, J.; Zdrahal, Z.; Vegrosta, J.; Chmelik, J. *J High Resol Chromatogr* 2000, 23, 502.
18. Chmelik, J.; Planeta, J.; Rehulka, P.; Chmelik, J. *J Mass Spectrom* 2001, 36, 760.
19. Dong, X.; Proctor, A.; Hercules, D. M. *Macromolecules* 1997, 30, 63.
20. Chercoles, A. R.; San, A. M. M.; de la Roja, J. M.; Gomez, M. *Anal Bioanal Chem* 2009, 395, 2081.
21. Tiwari, A.; Nema, A. K.; Das, C. K.; Nema, S. K. *Thermochim Acta* 2004, 417, 133.
22. Wright, N.; Hunter, M. J. *J Am Chem Soc* 1947, 69, 803.
23. Bonavoglia, B.; Storti, G.; Morbidelli, M. *Macromolecules* 2005, 38, 5593.
24. Bonavoglia, B.; Storti, G.; Morbidelli, M. *Ind Eng Chem Res* 2006, 45, 3335.
25. Van Heukelum, A.; Barkema, G. T.; Edelman, M. W.; Van der Linden, E.; De Hoog, E. H. A.; Tromp, R. H. *Macromolecules* 2003, 36, 6662.